`

Predicting Effective Propagation Velocities of Acoustic Signals Using an Ocean Circulation Model

M. A. Sorokin(https://orcid.org/0000-0001-8933-2834)[a,*], P. S. Petrov [a,**], D. D. Kaplunenko [a], A. A. Golov(https://orcid.org/0000-0002-7160-0076)[a], and Yu. N. Morgunov [a]

[a] *Il'ichev Pacific Oceanological Institute, Far Eastern Branch of Russian Academy of Sciences, Vladivostok, 690041 Russia*

**e-mail: mikhapilot@mail.ru*

***e-mail: petrov@poi.dvo.ru*

Abstract—The possibility of applying ocean circulation modeling data to forecast the effective velocities of pulse acoustic signal propagation from the continental slope to the deep ocean is studied. Prediction of these velocities is crucial for reliable operation of acoustic navigation and ranging systems, while typical lengths of paths and the prediction accuracy requirements almost completely exclude the use of direct measurements for this purpose. Analysis of experimental data obtained on a 200-km-long acoustic path shows that the NEMO ocean circulation model used for reconstruction of the sound speed distribution along this path allows one to calculate with sufficiently high accuracy the effective velocities of propagation of pulse acoustic signals transmitted by a source on the shelf and received in the deep-water part of the Sea of Japan. The proposed method for calculating the effective velocities is based on the adiabatic mode theory of sound propagation on the shelf, as well as on the fact that in the deep-water part of the path, the group velocities of low-number modes are very close to each other.

Keywords: shallow-to-deep scenario, pulse signal, arrival times, group velocities, acoustic ranging

INTRODUCTION

The development of acoustic navigation and ranging systems is among current research trends in ocean acoustics [1–3]. In the case of long-range acoustic navigation systems, one of key challenges related to positioning accuracy is to properly take into account the depth and range dependence of the environment in which acoustic signals propagate from the source to the reception point. <…> In this case, it is also necessary to consider into account the difference in the physical properties of the shallow- and deep-water waveguides when computing effective propagation velocities, as well as the presence of a transition region between them (the continental slope).

The fact that typical distances from the source to the receiver in problems of long-range acoustic navigation are hundreds of kilometers [1, 3–5], as well as the need for efficient velocity forecasting, completely rule out the possibility of using direct measurements as the method for computing the sound field distribution. As will be shown below, even in the case of hydrological measurements performed at several points on the path just before the experiment, the resulting information on effective velocity variations along the path is insufficient. For this reason, in average effective velocity forecasting, either global ocean circulation modeling systems (with the data assimilation) [1, 3], or a database where long-term measurements data is accumulated [6] should be used. In this paper, an example of successful application of the former technique is demonstrated.

We consider an experiment with the shallow-to-deep propagation scenario (Cape Shultz in the deep-water part of the Sea of Japan), performed by the Il'ichev Pacific Oceanological Institute (POI) in 2017. It is shown that the effective velocities for this experiment can be calculated using the sound speed in water column obtained from the NEMO global ocean circulation model. The effective velocities estimated from this data even allow us to calculate the arrival times of individual components of the pulse signal. These components correspond to the peaks on the waveguide impulse response function obtained in the experiment. In this article, we understand the waveguide impulse response function (IRF) as the modulus of the cross-correlation function of the emitted and received signals.

<…>

It is known that the acoustic energy in each waveguide cross section propagates with the group velocity of the modal components of the pulse acoustic signal [4, 5, 7]. For this reason, in the case of a range-independent waveguide, the arrival times of the IRF maxima strictly correspond to the quotient of the path length and these group velocities (e.g., calculated for the center frequency of the signal). In the case of a range-independent waveguide (especially in the "shallow-to-deep" scenario), the identity of modal components is gradually erased as they propagate along the path due to the redistribution of acoustic energy between them [7] (this process is usually called mode interaction/mode coupling). Nevertheless, the qualitative understanding and quantitative estimates presented in this work show that the impulse response peaks, obtained when transmitting a signal from the shelf and receiving it in the deep ocean, can be associated with the path-averaged group velocities of low-number modes.

This study is dedicated to a more accurate assessment of the effective propagation velocities of pulse signals (in comparison with [1, 5]), and it is organized as follows. In the second section, a description of a full-scale experiment is provided. The analysis of this experiment is performed in the remaining part of the article. In the third section, a waveguide model for this experiment is constructed using hydrological data (i.e., the sound speed distribution) obtained from the NEMO ocean circulation model [8]. The fourth section is dedicated to the description of a method for estimating effective propagation velocities (it was first outlined in our previous work [4, 9]) and its qualitative justification. Finally, in the fifth section, the comparison of arrival times calculated using estimated effective velocities with arrivals observed in the experiment is presented. This comparison confirms that the described technique makes it possible to obtain an adequate prediction of the IRF in a complex waveguide in the "shallow-to-deep" scenario.

EXPERIMENT AND AVAILABLE SOUND SPEED MEASUREMENT DATA

The experiment discussed in this article was conducted by POI FEB RAS in September 2017 on the acoustic path shown in Fig. 1a. At 150 m from the coastline at a depth of 34 m, a broadband piezoceramic transducer was deployed near the sea bottom. It transmitted complex phase-shift keyed signals once a minute (M-sequences 1023 symbols long, 4 carrier frequency periods per symbol) with a center frequency of 400 Hz. In what follows, we call this transducer a source of navigation signals (SNS). Signals were received in the deep-water part of the Sea of Japan at four points along the path at distances of about 68, 86, 90, and 198 km from the source.

In this work, we will consider only the IRF calculated for the receivers deployed at points 2 and 5, located 68 and 198 km from the SNS, respectively.

<…>

SOUND SPEED FIELD OBTAINED FROM THE NEMO MODEL

As can be seen from Fig. 2, the sound speed measurement points have uneven distribution along the path. For example, along the last 100 km, the sound speed distribution is obtained by linear interpolation by only two sound speed profiles (SSP). Obviously, in this case, there can be even a large-scale inhomogeneity between them (e.g., a synoptic eddy), which will not appear at all in the resulting distribution. The influence of inhomogeneities of this kind on sound propagation can be significant as discussed, e.g., in [9–11]. Obviously, the only measurement taken on the shelf section of the path also cannot provide detailed information on the sound speed variability along its entire length. On the other hand, in realistic conditions of acoustic navigation systems functioning, direct measurements of SSP can be performed only at the points of transmission and reception. Thus, information on the sound velocity field along the path will be even less accurate.

<…>

Currently, the most frequently used global models of ocean circulation in the problems of reanalysis and forecasting of the water column state are hybrid coordinate ocean model (HYCOM) [12] and nucleus for European modeling of the ocean (NEMO) [8, 13]. Both models are based on the numerical solution of the Navier–Stokes equations, and their main difference is in the z coordinate discretization (as the name suggests, the grid in the HYCOM model is hybrid and uses different mesh size in different layers of the water column). As noted above, the authors of [1, 3] used hydrological data obtained by the HYCOM model, which is usually used by US government organizations. In the present study, a preference to the NEMO model was given, since the obtained SSP estimates agree better with the available data of field measurements.

The sound speed distribution in the vertical plane containing the path under consideration obtained from the NEMO model is shown in Fig. 3. As seen from this figure, approximately 140 km from the beginning of the path, there is a large-scale inhomogeneity of the sound velocity field, which leads to a very characteristic “divergence” of its isolines. Apparently, in this case, we can talk about the presence of a synoptic eddy on the path section from 120 to 160 km from the SNS. Obviously, this eddy cannot be detected in the available hydrological sounding data. An altimetry map of the ocean surface, also constructed using the NEMO model (see Fig. 1b), confirms this conclusion. Obviously, not only the presence of this eddy on the path, but also its position and parameters can hardly be estimated from averaged long-term data of hydrological measurements. Of

`

course, this is just one of the most obvious examples of the refinement of information about the sound velocity field on the path under consideration.

METHODOLOGY FOR THE ESTIMATION OF EFFECTIVE PROPAGATION VELOCITIES OF THE SIGNAL COMPONENTS

It is possible to estimate the effective propagation velocities of individual modal components of pulsed acoustic signals using the following technique (see also [4, 5]) with experimental and model hydrological data usage (sound velocity fields in the vertical plane containing the path) presented in Figs. 2 and 3.

For the *j*th modal component of the sound field, the propagation of acoustic energy in the horizontal direction at a given point of the path *r* occurs with the group velocity of a given mode and in a presented waveguide cross-section can be calculated by the formula [7]

$$v_j^{g}(f) = \frac{d\omega}{dk_j} .$$

If modal functions ϕ_j and wavenumbers $k_j = k_j(r, \omega)$ are known, then the group velocity in each section of the waveguide can be calculated using the relation

$$\frac{1}{v_j^{g}(r)} = \frac{\omega}{k_j}\int_0^H \frac{(\phi_j(z))^2}{\rho(z)c^2(z)}dz.$$

The distance from the source to the receiver along the geodesic R_{GPS} and arrival time of *j*th modal component along the track t_j are linked with the following integral relation:

$$t_j = \int_0^{R_{GPS}} \frac{dr}{v_j^{g}(r)}. \quad (1)$$

This formula is inconvenient both for solving problems of acoustic ranging (for estimation of R_{GPS}) , and for arrival times t_j calculation, as R_{GPS} is placed in the upper limit of integral. To solve this kind of problem, we will use the auxiliary value

$$v_{eff}(j, f) = R_{GPS}/t_j, \quad (2)$$

– effective propagation velocity of *j*th modal component. For the calculation convenience the track is divided into *n* segments, and each of them corresponds to the ε_i portion from the total path length, i.e.. the ratio $(\varepsilon_1 + \varepsilon_2 + \ldots + \varepsilon_n) = 1$ is performed. If an effective velocity is v_{eff}^i on *i*th segment, the effective velocity in the whole track can be calculated using the equation

$$v_{eff} = \frac{1}{\sum_{i=1}^{n} \frac{\varepsilon_i}{v_{eff}^i}}. \quad (3)$$

<…>

SUBSTANTIATION OF THE METHOD: CHANGING THE MODAL STRUCTURE OF FIELD ALONG THE PAH

The acoustic waveguide shown in Figs. 2 and 3 can be divided into three parts, and each of them is characterized by different physics of acoustic wave propagation.

The initial shelf section of the path has a length of about 25 km. The depth along this section varies from 35 to 120 m, the angles of the bottom inclination exceed no more than 1° (the average angle of inclination throughout the entire section is only 0.2°). For this reason, sound propagation in this area occurs almost adiabatically [7, 14], and only a small part of the acoustic energy of *j*th modal component of the generated signal will be redistributed between other modes after passing through this section. On the other hand, in this section, the group velocities of various water modes differ quite strongly (see Table 1, where the average values of this quantity are calculated for the entire shallow water section and for a certain point close to its middle). For example, the difference in the velocities of the first and tenth modes at the center frequency of the pulse signal is about 35 m/s, and the first and fifth—about 10 m/s (and the dependence of the group velocity on the mode number is not monotonic).

<…>

ARRIVAL TIMES OF SIGNAL COMPONENTS: COMPARISON WITH EXPERIMENT

In this section our goal is to compare the IRF obtained from the experiment with the estimations of the individual signal components arrival times by the formula (5) on the considered path. The results of this comparison are shown in Figs. 4 and 5 for the receivers at distances of 68 and 198 km from the source, respectively (the plot from Fig. 4 for the sound velocity field constructed according to the NEMO model is also shown in Fig. 6 in more detailed way).

<…>

Let us now consider the graph shown in Fig. 4b (see also Fig. 6) in more detailed way. As can be seen, the theoretical arrival times (5), calculated from the path-averaged group velocities of individual modes (formulas (3)–(4)), can be associated with individual peaks of the IRF, which are highlighted in the graph by dotted circles, and their color corresponds to colors of associated peaks of modal components.

<…>

CONCLUSIONS

The paper studies the propagation of pulsed acoustic signals transmitted by a source on the shelf and received in the deep ocean USC. It is shown that in such propagation scenario, the signal is divided into several separate components, which correspond to the modes excited by the source in the shallow part of the path. Upon reaching the deep-sea part of the path, all these components (due to the intense mode coupling on the continental slope) get transformed into superpositions of USC modes with numbers 1–20. It is shown that the differences between the group velocities of modes 1–20 in the USC are one to two orders of magnitude smaller than the differences between the group velocities of modes 1–10 on the shelf. Consequently, when the signal propagates few hundred

`

kilometers in the USC, it still consists of the components with relative delays mostly determined by the intermodal dispersion on the shelf (i.e., they are very close to the relative delays of the modal components of the signal at the continental slope beginning). This argument justifies the use of the formulas (3) and (4) for calculating the effective propagation velocities of individual components of the pulse signal in the scenario of sound propagation from the shelf to the deep ocean. Although these formulas were originally obtained in the adiabatic approximation, it turns out that they are also applicable for a path on which there is a relatively short section with strong modal interaction. However, it is necessary to emphasize once again that in our case the signal components whose arrival times are determined by these formulas are the superpositions of multiple modes propagating in the USC with group velocities close to each other.

To the best of our knowledge, this study is the first case when correct values of effective velocities of a pulse signal propagation in the shallow-to-deep scenario were computed using the sound velocity field obtained from the NEMO ocean circulation model. Note that in recent works [1], colleagues from USA used data from the HYCOM model for similar purposes, but in their case both transmission and reception of signals were carried out in the deep ocean USC that was approximated by an effective range-independent waveguide, and the accuracy was found to be satisfactory (in practice it was implemented by averaging SSP along the path). In this sense, the results reported here can be considered a generalization of the technique used by the authors of [1] to a more complex propagation scenario.

It appears that the models of ocean circulation, which in recent years have demonstrated significant progress in the ability to predict the qualitative behavior and quantitative characteristics of the marine environment, are the most promising tool for forecasting effective signal propagation velocities required for solving problems of acoustic ranging and acoustic navigation.

In conclusion, we note that the multiplicity of IRF peaks is usually considered one of the main difficulties arising in the solution of acoustic ranging and acoustic navigation problems. Indeed, when designing algorithms for distance estimation, it is desirable to explicitly indicate which peak of the IRF should be used to identify arrival time. The described method for determining the effective velocities can simplify the matching of theoretically calculated arrival times with these peaks.

FUNDING

The presented study is performed within the state task of POI FEB RAS (AAAA-A17-117030110034-7 and AAAA-A20-120031890011-8) and by grant 12578-93 from the Russian Science Foundation.

CONFLICT OF INTEREST

The authors declare that they have no conflicts of interest.

`

REFERENCES

1. M. Wu, M. Barmin, R. Andrew, P. Weichman, A. White, E. Lavely, M. Dzieciuch, J. Mercer, P. Worcester, and M. Ritzwoller, J. Acoust. Soc. Am. **146**, 4754 (2019). https://doi.org/10.1121/1.5138606

2. Yu. N. Morgunov, A. A. Golov, S. I. Kamenev, and Yu. V. Matvienko, Acoust. Phys. **65** (6), 711 (2019). https://doi.org/10.1134/S1063771019060101

<…>

10. V. A. Akulichev, A. V. Burenin, S. Yu. Ladychenko, V. B. Lobanov, and Yu. N. Morgunov, Dokl. Earth Sci. **475**, 942 (2017). https://doi.org/10.1134/S1028334X17080116

11. D. V. Makarov, L. E. Kon'kov, and P. S. Petrov, Izv. Vyssh. Uchebn. Zaved., Radiofiz. **59** (7), 638 (2016).

12. R. Bleck, Ocean Modelling **4** (1), 55 (2002). https://doi.org/10.1016/S1463-5003(01)00012-9

13. G. Madec and M. Imbard, Climate Dynamics **12**, 381 (1996). https://doi.org/10.1007/BF00211684

14. B. G. Katsnelson, V. G. Petnikov, and J. F. Lynch, *Fundamentals of Shallow Water Acoustics* (Springer, Heidelberg, 2012).

15. O. E. Gulin, Acoust. Phys. **54** (4), 495 (2008). https://doi.org/10.1134/S106377100804009X

16. F. D. Tappert, J. L. Spiesberger, and M. A. Wolfson, J. Acoust. Soc. Am. **111**, 757 (2002). https://doi.org/10.1121/1.1432983

17. D. V. Makarov, L. E. Kon'kov, M. Yu. Uleysky, and P. S. Petrov, Phys. Rev. E **87** (1), 012911 (2013). https://doi.org/10.1103/PhysRevE.87.012911

TABLES

Table 1. Group velocities of first 10 modal components of acoustic signal, calculated for ranges r = 0 km (SNS), r = 11.74 km (in middle of shelf part of waveguide) and averaged over shallow part of waveguide

Mode number j	1	2	3	4	5	6	7	8	9	10
R = 11.74 km	1455.6	1454.6	1455.0	1460.3	1467.0	1468.8	1458.4	1443.2	1427.2	1409.9
R = [0…20] km	1456.0	1455.4	1455.1	1460.2	1464.3	1458.9	1452.7	1443.6	1427.4	1410.1

<…>

`

FIGURE CAPTIONS

Fig. 1. (a) Schematic of experiment (2017) on pulse acoustic signal propagation in shallow-to-deep scenario (sound speed profiles along acoustic path are also shown), (b) ocean surface altimetry in experimental area obtained using NEMO model. Color represents deviation of ocean surface relative to geoid. Acoustic path is depicted by a sequence of black markers.

Fig. 2. Experimental hydrological data. Dotted lines indicate points at which hydrological measurements were made. (a) Deep-water part, (b) shallow water.

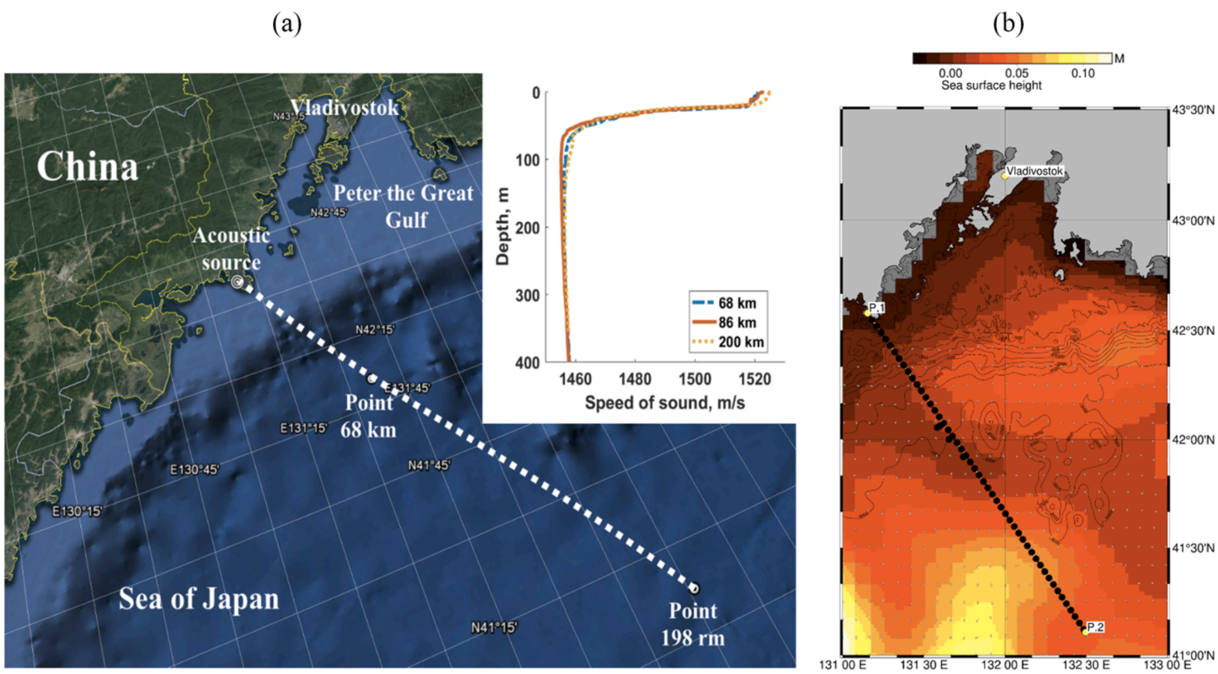

Fig. 1.

<…>